

Puzzling laminar (3) or "zonar" structures (5) resembling the concentric lamellae that I observed have been seen in scanning electron micrographs of fractured echinoid plates. A scanning electron micrograph of a broken trabecular bar from a young urchin (16) shows jagged structures that resemble crystallites, and Pearse and Pearse (16) suggest that organic material might be contained between lamellae. Theoretical (17) and x-ray diffraction (18) evidence also indicate polycrystallinity.

Some of the enigmatic features of echinoderm calcite can be explained if the polycrystalline model is typical of echinoderms. Crystallite lamellae may contribute to the strength of the stereom in two ways. (i) The crystallites are whisker-like and may share some of the strength properties (19) of whisker crystals. (ii) Since the outer trabecular surfaces are tightly packed cleavage faces, they are extremely smooth. The surface perfection of the trabeculae may produce strengthening by crack inhibition (3, 7, 8). The *Echinaster* material demonstrated loss of this surface smoothness at areas where stress concentrations were likely (Fig. 2C, arrows).

The curvature of the lamellae may explain the high  $Mg^{2+}$  concentration of echinoderm calcite. A smooth, curved surface cannot be formed from calcite crystals, which are rhombohedral, because the outer circumference must be greater than the inner circumference. The ionic radius of  $Mg^{2+}$  (0.67 Å) (12) is 32 percent smaller than that of  $Ca^{2+}$  (0.98 Å) (12), and magnesian calcites have smaller interplanar spacings in the crystal lattice (20). If the magnesium ions are located within the crystallites so that the inner faces are slightly contracted, the crystallites would fit together smoothly. Where the curvature is greatest—around tight curves and near the central axis— $Mg^{2+}$  would be more abundant than in the straighter sections of lamellae. Overall  $Mg^{2+}$  content varies among the different skeletal elements (6), but it is not known whether  $Mg^{2+}$  content varies with any of the smaller structural features such as lamellae.

All echinoderm ossicles are bound by connective tissue of some sort (21). Since the ossicle-dermis junction appears to be sensitive to loading rate, failure to observe crystallites in other studies may have been the result of producing fractures by rapid compression.

PATRICIA L. O'NEILL\*

Department of Zoology,  
Duke University,  
Durham, North Carolina 27706

## References and Notes

1. K. E. Chave, *J. Geol.* **62**, 266 (1952).
2. L. Klein and J. D. Currey, *Science* **169**, 1209 (1970).
3. D. Nichols and J. D. Currey, in *Cell Structure and Its Interpretation*, S. M. McGee-Russell and K. F. A. Ross, Eds. (Arnold, London, 1968), pp. 251–261.
4. G. Donnay and D. L. Pawson, *Science* **166**, 1147 (1969).
5. H.-U. Nissen, *ibid.*, p. 1150.
6. D. M. Raup, in *Physiology of Echinodermata*, R. A. Boolootian, Ed. (Wiley, New York, 1966), pp. 379–395.
7. J. D. Currey, in *Mechanical Design in Organisms*, S. A. Wainwright *et al.*, Eds. (Wiley, New York, 1976), p. 218.
8. D. Nichols, *Echinoderms* (Hutchinson, London, 1969), pp. 123–125.
9. Measurements were taken from the scanning electron micrograph negatives, 75 by 95 mm, which were magnified ( $\times 5$ ) with a photographic enlarger. Linear measurements were taken from the image with vernier calipers to the nearest 0.1 mm; measurements could be repeated within  $\pm 10$  percent ( $N = 50$ ). Since it was not possible to correct for perspective, the measurements are approximate.
10. Angular measurements, taken from enlarged negatives (9), were read by use of a protractor with a vernier scale to the nearest 0.1° and rounded to the nearest degree. Care was taken to minimize perspective and parallax, although error is unavoidable in measuring a three-dimensional object in two dimensions. Angular measurements could be repeated within 0.8° ( $N = 25$ ).
11. E. S. Dana and W. E. Ford, *Dana's Manual of Mineralogy* (Wiley, New York, ed. 16, 1952), p. 265.
12. W. A. Deer, R. A. Howie, J. Zussman, *Rock-Forming Minerals*, vol. 5, *Non-Silicates* (Wiley, New York, 1962), pp. 227–255.
13. All scanning electron microscopy specimens were fractured during mechanical testing (14). Those not immediately prepared for microscopy were stored in buffered 10 percent formalin. Specimens were dipped in distilled water to remove sea salts, then air-dried under cover for 1 week. They were then coated with 200 Å of gold-palladium and examined with a JEOL scanning electron microscope.
14. Test sections were cut from the dorsal body wall of a sea star; the ossicles were loaded indirectly by pulling on the collagenous portion of the body wall. For fast fractures, the sea star was unanesthetized. The specimens were clamped into a mechanical testing machine with two rubber-padded screw clamps. One clamp was attached to a fixed carriage and the other to a sliding carriage with braided wire and binding posts. The position of the sliding carriage was adjusted with a thumbscrew that allowed the specimen to be stretched and fractured. Displacement was monitored by two colinear linear variable differential transformers whose cores were attached to the specimen by two needle points. Force output was delivered by a strain gauge on a cantilever fixed to the stationary carriage mount. Force and displacement were recorded on a Brush dual-pen recorder. Fast fracture specimens were loaded in tension at an elongation rate of about 1 percent per second until fracture. The specimens were irrigated with artificial seawater (Instant Ocean) during testing. For stress relaxation, the sea stars were anesthetized in 0.1 percent MS-222 in artificial seawater for 1 hour before the test sections were cut. The sections were irrigated with the same solution during the experiment. The MS-222 was necessary to prevent muscle contraction, which deformed the specimen, although no differences in fracture surfaces were apparent in stress-relaxed specimens that were not treated with MS-222. The specimens were placed in the mechanical testing machine and loaded in tension at 3 to 8 MN/m<sup>2</sup>. Force was continuously recorded; when the force had decayed to near 0, usually after about 10<sup>3</sup> seconds, the specimen was pulled at an elongation rate of about 1 percent per second until it was fractured.
15. The ossicles lie within a collagenous dermis to which they are firmly attached by collagen fibers that project through holes in the stereom.
16. J. S. Pearse and V. B. Pearse, *Am. Zool.* **15**, 731 (1975).
17. K. M. Towe, *Science* **157**, 1048 (1967).
18. H. U. Nissen, *Neues Jahrb. Geol. Palaeontol. Abh.* **117**, 230 (1963).
19. S. S. Brenner, in *Fiber Composite Materials* (American Society for Metals, Metals Park, Ohio, 1965), pp. 11–36.
20. J. R. Goldsmith, D. L. Graf, O. I. Joensuu, *Geochim. Cosmochim. Acta* **7**, 212 (1955).
21. L. H. Hyman, *The Invertebrates*, vol. 4, *Echinodermata* (McGraw-Hill, New York, 1955), p. 4.
22. I thank S. Wainwright for his assistance, enthusiasm, and encouragement during this study. J. Hebrank designed and built the mechanical testing machine, which I modified for use in this work. Supported by research funding and a postdoctoral fellowship from the Cocos Foundation, Inc.  
Present address: Department of Biology, Portland State University, Box 751, Portland, Ore. 97207.

18 December 1980; revised 22 April 1981

## Quiet Zone Within a Seismic Gap near Western Nicaragua: Possible Location of a Future Large Earthquake

**Abstract.** A 5700-square-kilometer quiet zone occurs in the midst of the locations of more than 4000 earthquakes off the Pacific coast of Nicaragua. The region is indicated by the seismic gap technique to be a likely location for an earthquake of magnitude larger than 7. The quiet zone has existed since at least 1950; the last large earthquake originating from this area occurred in 1898 and was of magnitude 7.5. A rough estimate indicates that the magnitude of an earthquake rupturing the entire quiet zone could be as large as that of the 1898 event. It is not yet possible to forecast a time frame for the occurrence of such an earthquake in the quiet zone.

Segments of seismically active plate boundaries in the circum-Pacific that have not been ruptured by a large (magnitude  $M$  greater than 7) earthquake for 30 years or more are considered likely locations for future large earthquakes (1, 2). The earthquake potential of each segment, or "seismic gap," is considered to increase with the time since the last large earthquake within that segment. Since 1973, when this concept was presented

by Kelleher *et al.* (1), nearly all large circum-Pacific earthquakes have occurred within such gaps. The concept has been of great utility in forecasting where large earthquakes should occur. To be socially useful, however, earthquake predictions must specify the time of these events more accurately. Some workers (3) have reported precursory patterns of seismicity that may make possible the forecasting of large

earthquakes to within a few years. Typically, a large part of the future rupture zone is seismically quiescent for years to decades compared to adjacent regions; then, in the months to years before the main shock, seismicity increases in the area immediately surrounding the quiet zone. Although the details of such precursory seismicity are limited by the poor quality of available data, a successful forecast (4) of the recent large earthquake near Oaxaca, Mexico (29 November 1978,  $M = 7.9$ ), was based on similar changes in seismicity. These observations suggest that it may be possible to pinpoint the locations of some future large earthquakes by searching delineated seismic gaps or regions of high seismic potential for quiet zones surrounded by areas of increasing seismic activity. We investigated such a zone of seismic quiescence that appears in earthquake location data from a new seismograph network in western Nicaragua.

The Nicaraguan network, installed as a cooperative project between the government of Nicaragua and the U.S. Geological Survey, consists of 16 remote high-gain seismograph stations that have been operating since April 1975. Seismic signals from 1-Hz seismometers at each station are relayed by very high frequency radio to the offices of the Instituto de Investigaciones Sísmicas (IIS) in Managua, Nicaragua, where they are recorded on 16-mm film. For each earthquake the arrival times and signal duration at individual stations are determined and the hypocenter, origin time, and magnitude are calculated by computer. A detailed description of the instrumentation and data reduction methods has been published (5). The precision of earthquake epicenters calculated with the Nicaraguan data is better than 5 km. Between April 1975 and December 1978 more than 4000 earthquakes were located with data from the network, compared to only 45 events recorded teleseismically. The new seismograph network, therefore, enables the rapid accumulation of precise earthquake locations for western Nicaragua.

Most earthquakes along the Pacific coast of Nicaragua originate along the seismically active plate margin and result from the northeasterly underthrusting of the Cocos plate beneath the Caribbean plate (6). Preliminary results from Nicaragua (5) show that seismicity is primarily confined to a 15- to 25-km-thick slab, or subduction zone, striking roughly parallel to the coastline and dipping north-eastward from the surface at the Middle America trench to a depth of about 200 km beneath a chain of active volcanoes.

Analysis of the high-quality Nicaraguan data reveals an area of seismic quiescence down to magnitude 2 at shallow depth on the subduction zone (Fig. 1). This quiet zone is approximately 50 km wide parallel to the coastline and extends 115 km downdip on the subduction zone to a depth of about 50 km.

Although narrow compared to the rupture widths of large subduction zone earthquakes, whose longest dimension is usually parallel to the strike of the subduction zone, the Nicaraguan quiet zone is similar to the rupture zones of several large Central American earthquakes that also have a longer downdip dimension (1, 2, 7). This quiet zone lies inside the southeast end of a seismic gap identified by Kelleher *et al.* (1) that extends 400 km along the Pacific coasts of El Salvador and northwestern Nicaragua (see inset in

Fig. 1). McCann *et al.* (2) assign this gap a seismic potential of category 2, corresponding to a region that has produced a large earthquake more than 30 but less than 100 years ago. They consider that this gap may be the site of a large earthquake within a few years to a few decades, because the time since the last large earthquakes within the gap region, which occurred in 1921 ( $M = 7.3$ ) and 1926 ( $M = 7.1$ ), is roughly equal to the 50-year average recurrence interval for large earthquakes in Central America. At least six earthquakes of magnitude 7 or larger have occurred within the present seismic gap since 1850 (8). Each of these events, however, ruptured only a portion of the gap region, suggesting that, in the future, the gap will be ruptured by several large earthquakes rather than one great earthquake. We therefore consider

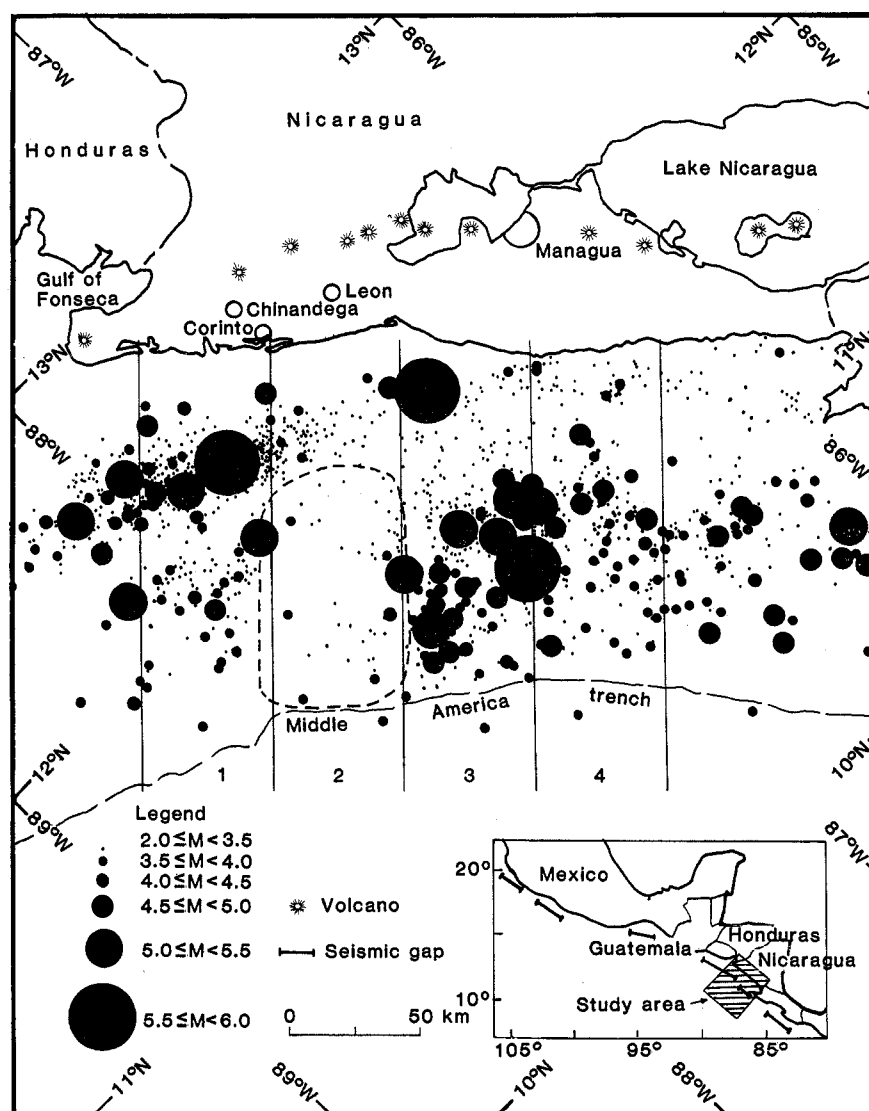


Fig. 1. Epicenter map of the upper 70 km of the subduction zone, containing two data sets: the smallest circles represent 1000 events of  $2.0 \leq M < 3.5$  recorded between April 1975 and June 1978; all larger circles represent events of  $M \geq 3.5$  recorded between April 1975 and December 1978. The dashed line shows the location of the quiet zone. (Inset) Location of map area (shaded box) and locations (bars) of Central American seismic gaps identified by Kelleher *et al.* (1).

that the quiet zone, which lies inside the El Salvador–Nicaragua seismic gap, may be the specific site of one of these future large earthquakes.

We searched the available teleseismic records of earthquakes and the historical accounts for evidence of previous large earthquakes in the vicinity of the quiet zone. A relocation study of teleseismically recorded earthquakes near Nicaragua for the period 1950 through 1972 by Dewey and Algermissen (9) reduced location errors to a maximum of 10 to 20 km. Inspection of the results indicates a quiet zone of similar dimensions in the midst of earthquakes of magnitude 5 and larger since at least 1950, at the same location as that revealed by the new local data. The most recent destructive shallow earthquake in the vicinity of the quiet zone was recorded on 29 April 1898 with a magnitude of 7.5 (10). This earthquake must have ruptured the quiet zone because Rossi-Forel intensities of V to IX were reported between Managua and the Gulf of Fonseca (11). The greatest damage occurred in Leon, Chinandega, and Corinto—cities directly onshore from the present quiet zone. Historical accounts of earthquakes prior to 1898 are sketchy; earthquakes that may have originated in this area in 1850, 1881, and 1885 (12) appear to have been significantly smaller. The 1898 earthquake indicates that, although the Nicaraguan quiet zone has existed since at least 1950, it is not permanently aseismic and that this region is capable of producing a magnitude 7.5 earthquake. The 82-year period since the 1898 earthquake is long compared to the average recurrence interval of 50 years for large earthquakes in Mexico and Central America (1, 2), suggesting that a large earthquake in this area might be long overdue or that aseismic slip plays an important role in accommodating plate motion. The paucity of historical data prior to 1898, however, makes it difficult to determine whether there are large fluctuations in the recurrence intervals or whether the recurrence interval for this area might be longer.

Reported seismicity patterns preceding large earthquakes are diverse and their usefulness as a predictor is still uncertain (13). One pattern observed is an increase in seismic activity along the edges of a zone of quiescence before the main shock (3). To examine changes in seismicity with time, we divided the seismically active coastal region of Nicaragua into four 50-km-wide segments, one of which was centered on the quiet zone (Fig. 1). In Fig. 2, the distribution of earthquakes with time for each segment

is plotted for locally recorded earthquakes larger than magnitude 3.5 between 1975 and 1978 and for teleseismically recorded earthquakes of magnitude 5.0 and larger from 1950 to 1978. Data from 1979 and 1980 were not used because interruptions in network operations and data processing due to the recent civil war in Nicaragua resulted in an uneven data set for that period. In Fig. 2a, an increase in the number of earthquakes of magnitude 3.5 and larger appears in mid-1977 for the segments on each side of the quiet zone. A count of earthquakes indicates that during the 1.5 years after mid-1977, 81 events of magnitude 3.5 and larger occurred along the edges of the quiet zone, compared to only 25 events during the preceding 1.5 years. Part of this increased seismicity, however, is due to large aftershock sequences following two moderate-sized earthquakes on 31 May 1978 (body-wave magnitude  $M_b = 5.7$ ) and 19 December 1978 ( $M_b = 5.3$ ) that occurred on the northwest and southeast edges, respectively, of the quiet zone. In addition, the distribution of earthquakes of magnitude 5.0 and larger (Fig. 2b) during 1975 through 1978 is not significantly different

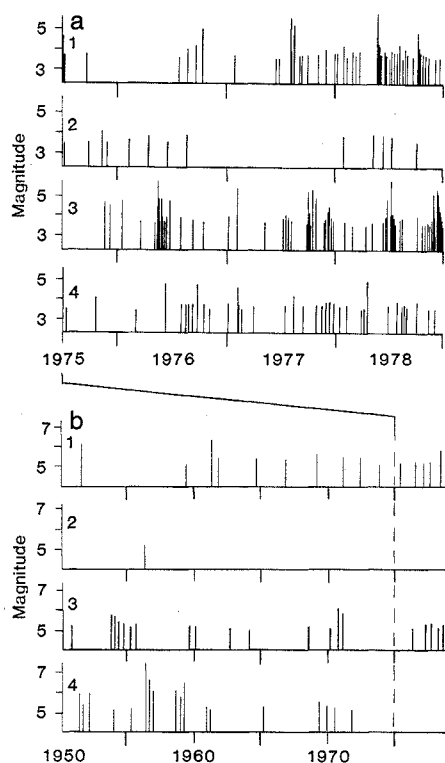


Fig. 2. (a) Space-time distribution of  $M \geq 3.5$  earthquakes for four adjacent 50-km-wide segments along the strike of the Nicaraguan subduction zone. Segment 2 is centered on the quiet zone (see Fig. 1). Data were recorded by the Nicaraguan seismic network between April 1975 and December 1978. (b) Space-time distribution of  $M \geq 5$  earthquakes since 1950, using the epicenters relocated by Dewey and Algermissen (9).

from the overall distribution of these events since 1950. Therefore the increase in the number of smaller earthquakes along the edges of the quiet zone since mid-1977 may be a normal fluctuation in the level of seismicity.

We can estimate the magnitude of an earthquake rupturing the entire quiescent area from a calculation of the seismic moment,  $M_0$ , given by  $M_0 = \mu uA$ , where  $\mu$  is the shear modulus,  $7 \times 10^{11}$  dyne/cm<sup>2</sup> [an average value for the mantle (14)];  $A$  is the area of the quiet zone, 5700 km<sup>2</sup>; and  $u$  is the average potential slip on the fault during an earthquake. Potential fault slip, however, is not well constrained because the percentage of strain released seismically is not well known. One study indicates that 25 to 90 percent of the strain is released seismically along circum-Pacific subduction zones (15). Thus a potential fault slip can be approximated by using 25 percent seismic strain release, a plate convergence rate of 8.4 cm/year (16), and the duration of strain accumulation. A minimum value for duration is 30 years, the length of time for which the quiet zone has been definitely known to exist. The resulting fault slip is 0.6 m. If we use duration as the time since the 1898 earthquake, we obtain a maximum fault slip of 1.7 m. Fault slips of 0.6 and 1.7 m yield respective seismic moments of  $2.4 \times 10^{27}$  and  $6.8 \times 10^{27}$  dyne-cm or corresponding magnitudes of 7.6 and 7.9 (17). Although the uncertainties in estimating the magnitude of a future earthquake can be large, these estimates indicate that an earthquake similar to the magnitude 7.5 earthquake of 1898 could be produced in the quiet zone.

Some idea of the damage that could be expected from such an earthquake may be obtained from damage reports of previous earthquakes. The 1898 earthquake damaged hundreds of homes and some buildings, many beyond repair, in the towns and cities along the Pacific coast (12). The greatest damage was to taquezal-type buildings and homes, which are still common in western Nicaragua. Taquezal construction consists of a wood-post frame, wood-lath and adobe walls, and a heavy tiled roof. This type of construction has little resistance to lateral shear stresses generated by an earthquake (18). Thus an earthquake of about magnitude 7.5 in the quiet zone poses a significant risk to life and property in the cities and area of Leon, Chinandega, and Corinto, Nicaragua's principal port.

In summary, earthquake data from a new high-gain seismograph network reveals a 5700-km<sup>2</sup> area of seismic quiescence on the shallow subduction zone

near the Pacific coast of Nicaragua. The quiet zone lies within a region indicated by the seismic gap technique to be a likely location for an earthquake of magnitude 7 or larger within the next few decades. Teleseismic data show that the quiescence has existed since at least 1950 and that the quiet zone appears to have been last ruptured by a magnitude 7.5 earthquake in 1898. Because the rupture zones of large earthquakes are observed to be seismically quiescent for years to decades prior to the main shock, the quiet zone in Nicaragua may be the site of a future large earthquake. A rough estimate of the magnitude of an earthquake that would rupture the entire quiet zone indicates that it could be comparable to the magnitude 7.5 event in 1898.

An increase in the level of seismicity in the magnitude range 3.5 to 5.0 occurred along the edges of the quiet zone in mid-1977 and continued through 1978. The distribution of earthquakes of magnitude 5.0 and larger for the same time period, however, is not significantly different from the overall distribution of earthquakes larger than magnitude 5.0 since 1950. Thus it is not known whether the increase in the number of magnitude 3.5 to 5.0 events is a normal fluctuation in lower magnitude seismicity or part of a precursory pattern. Moreover, observed precursory seismicity patterns vary and their use as a predictor is still in the development stage. We feel, therefore, that although the data clearly show a seismic quiet zone that is a possible location for a future large earthquake, they do not yet enable forecasting of such an earthquake within a specific time frame.

DAVID H. HARLOW

RANDALL A. WHITE

INES LUCIA CIFUENTES

U.S. Geological Survey,  
Menlo Park, California 94025

ARTURO ABURTO Q.

Instituto de Investigaciones Sísmicas,  
Managua, Nicaragua

#### References and Notes

1. J. A. Kelleher, L. R. Sykes, J. Oliver, *J. Geophys. Res.* **78**, 2547 (1973).
2. W. R. McCann, S. P. Nishenko, L. R. Sykes, J. Krause, *U.S. Geol. Surv. Open-File Rep.* 78-943 (1978), p. 441.
3. K. Mogi, *Bull. Earthquake Res. Inst. Tokyo Univ.* **47**, 395 (1969); J. A. Kelleher and J. Savino, *J. Geophys. Res.* **80**, 260 (1975).
4. M. Ohtake, T. Matumoto, G. V. Latham, *Pure Appl. Geophys.* **115**, 375 (1977).
5. A. Aburto, *Bull. I.I.S. (Inst. Invest. Sísmicas) Managua, Nicaragua* **1** (1975).
6. P. Molnar and L. R. Sykes, *Geol. Soc. Am. Bull.* **80**, 1639 (1969); B. W. Dean and C. L. Drake, *J. Geol.* **86**, 111 (1978).
7. S. K. Singh, J. Havskov, L. Ponce, K. McNally, L. Gonzalez, *Earthquake Notes* **49**, 49 (1979).
8. M. J. Carr and R. E. Stoiber, *Geol. Soc. Am. Bull.* **88**, 151 (1977).
9. J. W. Dewey and S. T. Algermissen, *Bull. Seismol. Soc. Am.* **64**, 1033 (1974).
10. H. Kanamori and K. Abe, *J. Geophys. Res.* **84**, 6131 (1979).
11. J. Crawford, *Am. Geol.* **22**, 56 (1898).
12. F. Montessus de Ballore, *Tremblements de Terre et Éruptions Volcaniques au Centre-Amérique Depuis la Conquête Espagnole Jusqu'à Nos Jours* (Société des Sciences Naturelles de Saône-et-Loire, Dijon, 1888).
13. M. Ohtake, T. Matumoto, G. V. Latham, *Bull. I.I.S. (Inst. Invest. Sísmicas) Earthquake Eng.* **15**, 105 (1977); E. R. Engdahl, *U.S. Geol. Surv. Open-File Rep.* 79-943 (1978), p. 163; L. M. Jones and P. Molnar, *J. Geophys. Res.*, in press; M. Reyners, in *3rd Maurice Ewing Symposium—Earthquake Prediction*, D. W. Simpson and P. G. Richards, Eds. (American Geophysical Union, Washington, D.C., in press), vol. 4.
14. P. Molnar, *Bull. Seismol. Soc. Am.* **69**, 115 (1979).
15. L. R. Sykes and R. C. Quittmeyer, *Eos* **60**, 884 (1979).
16. J. B. Minster and T. H. Jordan, *J. Geophys. Res.* **83**, 5331 (1977).
17. H. Kanamori, *ibid.* **82**, 2981 (1977).
18. L. A. Wyllie, Jr., R. N. Wright, M. A. Sozen, H. J. Kegenkoib, K. V. Steinbruggen, S. Kramer, *Bull. Seismol. Soc. Am.* **64**, 1069 (1974).
19. We thank A. G. Lindh, W. Thatcher, P. L. Ward, and D. M. Boore for critically reading this report. We especially thank D. Fajardo and co-workers at the Instituto de Investigaciones Sísmicas in Managua for their diligence in maintaining the seismic network and analyzing the seismograms.

11 February 1981

## Spectral Analysis of Tropospheric Aerosol Measurements Obtained with a New Fast Response Sensor

**Abstract.** A new fast response sensor was used in aircraft studies of fluctuations in the size distributions of tropospheric aerosol and their relation to fluctuations of trace gas concentrations and light scattering coefficients. Spectral analysis of data upwind of Buffalo, New York, and Houston, Texas, suggests important roles for atmospheric turbulence and chemical reaction in aerosol fluctuations.

Essential information on the dynamical processes governing the tropospheric aerosol is contained in the smaller scale spatial and temporal fluctuations in the particle size distribution. Despite extensive investigations of the tropospheric (principally urban) aerosol over the past decade [for example (1)], these fluctuations and their relation to fluctuations in trace gas concentrations and light transmission have received little attention. In this report we present a detailed analysis of these phenomena that was made possible by our development of an instrument called the electronic cascade impactor (ECI) to obtain information on the aerosol size distribution in real time (2). The measurement systems used in our aircraft studies and the spectral techniques employed in our analysis are briefly described. Typical conditions and a few representative results are given for the spectral relation among aerosol size fractions, trace gas concentrations, and light scattering coefficients.

The data for the spectral analyses were obtained from separate field studies in Buffalo, New York, during 24 to 31 March 1980 and Houston, Texas, during 5 to 15 June 1980. Although different aircraft were used, the quantities measured were the same: particle size distribution (ECI channels), trace gas concentration ( $\text{SO}_2$ ,  $\text{O}_3$ ,  $\text{NO}_x$ ,  $\text{NO}$ ,  $\text{NO}_2$ ), light scattering coefficient  $b_s$  (integrating nephelometer), pressure, and temperature. Data were digitized and recorded by data acquisition systems. All instruments, with the exception of the ECI, met Environmental Protection Agency (EPA) standards and were calibrated dai-

ly by standard procedures. The ECI was calibrated in the laboratory before and after each study; no changes were found in calibration.

In these studies the ECI permits determination of a large portion of the aerosol size distribution with response times under 1 second. In the ECI, aerosol particles acquire a positive electric charge from a corona charger. They then enter a multistage cascade impactor in which each impaction stage and the final filter are isolated electrically from other parts of the impactor and connected to an electrometer amplifier. Particles are collected on surfaces at different stages according to their aerodynamic diameter, as in an ordinary impactor, but the currents arising from the deposited charge can be measured, amplified, and recorded in real time and converted through suitable inversion techniques to give particle size distributions. Since a detailed description of the ECI was published (2), some changes in the instrument have been made. The ECI now in use is a seven-channel instrument having six impaction stages and a final filter. Impaction stages 1 through 6 have 50 percent aerodynamic cutoff diameters,  $D_{50}$ 's, of 9.6, 2.9, 1.1, 0.7, 0.42, and 0.25  $\mu\text{m}$ , respectively, while the final filter (ECI channel 7) gives the particle concentration below 0.25  $\mu\text{m}$  and correlates well (correlation coefficient,  $r = .95$ ) with a condensation nuclei counter (2).

Spectral analysis is a useful technique for examining the data from these aircraft field studies. While calculations of the mean, variance, auto-, and cross-correlation for the measured quantities